Vibrational spectroscopic study of the uranyl selenite mineral derriksite Cu$_4$UO$_2$(SeO$_3$)$_2$(OH)$_6$·H$_2$O

Ray L. Frost [a,*], Jiří Čejka [b], Ricardo Scholz [c], Andrés López [a], Frederick L. Theiss [a], Yunfei Xi [a]

[a] School of Chemistry, Physics and Mechanical Engineering, Science and Engineering Faculty, Queensland University of Technology, GPO Box 2434, Brisbane Queensland 4001, Australia
[b] National Museum, Václavské náměstí 68, CZ-115 79 Praha 1, Czech Republic
[c] Geology Department, School of Mines, Federal University of Ouro Preto, Campus Morro do Cruzeiro, Ouro Preto, MG 35400-00, Brazil

HIGHLIGHTS

- We have studied the mineral derriksite Cu$_4$UO$_2$(SeO$_3$)$_2$(OH)$_6$·H$_2$O.
- A comparison was made with the other uranyl selenites.
- Namely demesmaekerite, marthozite, larisaite, haynesite and piretite.
- Approximate U–O bond lengths in uranyl and O–H···O hydrogen bond lengths were calculated.

GRAPHICAL ABSTRACT
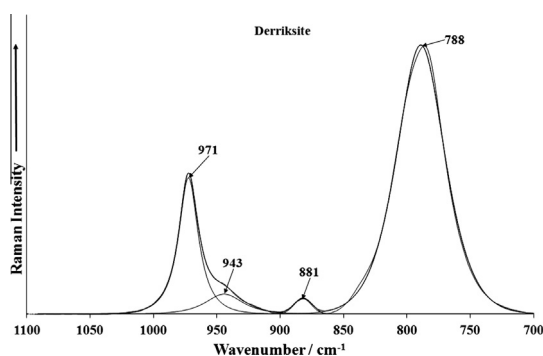
ABSTRACT

Raman spectrum of the mineral derriksite Cu$_4$UO$_2$(SeO$_3$)$_2$(OH)$_6$·H$_2$O was studied and complemented by the infrared spectrum of this mineral. Both spectra were interpreted and partly compared with the spectra of demesmaekerite, marthozite, larisaite, haynesite and piretite. Observed Raman and infrared bands were attributed to the (UO$_2$)$^{2+}$, (SeO$_3$)$^{2-}$, (OH)$^-$ and H$_2$O vibrations. The presence of symmetrically distinct hydrogen bonded molecule of water of crystallization and hydrogen bonded symmetrically distinct hydroxyl ions was inferred from the spectra in the derriksite unit cell. Approximate U–O bond lengths in uranyl and O–H···O hydrogen bond lengths were calculated from the Raman and infrared spectra of derriksite.

© 2013 Elsevier B.V. All rights reserved.

Introduction

The crystal chemistry of selenium(IV) oxo-compounds shows great structural versatility expressed by the great number of different compounds [1]. Crystallochemical systematics of selenites was presented by Serezhkina et al. [2].

Uranyl anion topology of uranyl natural and synthetic compounds inclusive of uranyl selenites has been elaborated by Burns [3–6]. According to Finch and Murakami [7], uranyl selenites occur where Se-bearing sulfide minerals are undergoing oxidation and dissolution. Derriksite, demesmaekerite, guilleminite and marthozite are from the Musonoi Cu–Co mine, near Kalwezi, Katanga Province, Democratic Republic of Congo, piretite and also guilleminite from Shinkolobwe, Katanga Province, Democratic Republic of Congo, haynesite and larisaite from the Repete mine, San Juan Co., Utah, U.S.A [8,9].

Structures of derriksite, $Cu_4UO_2(SeO_3)_2(OH)_6 \cdot H_2O$ [10,11], and demesmaekerite, $Pb_2Cu_5[(UO_2)(SeO_3)_3]_2(OH)_6 \cdot (H_2O)_2$, are characterized by infinite chains formed from uranyl and selenite ions [6,12], while those of the remaining uranyl selenite minerals, guilleminite, $Ba[(UO_2)_3O_2(SeO_3)_2] \cdot (H_2O)_3$ [13], marthozite, $Cu[(UO_2)_3O_2(SeO_3)_2](H_2O)_8$ [14], larisaite, $Na(H_3O)[(UO_2)_3(SeO_3)_2O_2](H_2O)_4$ [9] and probably also haynesite, $[(UO_2)_3(SeO_3)_2(OH)_2] \cdot (H_2O)_5$ [15,16] and piretite, $Ca[(UO_2)_3(SeO_3)_2(OH)_4] \cdot (H_2O)_4$ [16] by uranyl oxo-hydroxo selenite sheets and phosphuranylite anion sheet topology. According to Chukanov et al. [9], the general formula of the minerals guilleminite, marthozite, haynesite, piretite and larisaite is $M_{0-1}[(UO_2)_3(SeO_3)_2(O,OH)_{2-4}] \cdot nH_2O$, where $a = 3–8$, $M = M^{2+}$, $2M^+$. In derriksite, the uranyl coordination polyhedra are formed from tetragonal (square) dipyramids UO_2O_4, in demesmaekerite pentagonal dipyramids UO_2O_5, and probably in all remaining natural uranyl selenites from pentagonal and hexagonal dipyramids UO_2O_5 and UO_2O_6, respectively similarly as in phosphuranylite. According to Ginderow and Cesbron [11], derriksite contains the brucite-type layers of CuO_6. Derriksite is structurally related to deloryite, $Cu_4(UO_2)(MoO_4)_2(OH)_6$ and the difference in space group between the two minerals is the direct consequence of the replacement of the SeO_3 trigonal pyramids in derriksite by the MoO_4 tetrahedra in deloryite. Deloryite does not contain any molecular water. This differs from derriksite containing one water molecule. Ginderow and Cesbron [11] inferred from thermogravimetric curve (TGA) presented by Cesbron et al. [10], that the first dehydration step (up to approximately 300 °C) may be connected with adsorbed water. However, the original Cesbron's interpretation that this first TGA step corresponds with one molecule of water of crystallization [10] seems to be more correct.

Raman spectroscopy was proven most useful for the characterization of secondary uranyl containing minerals [17–23]. The aim of this research is the study of Raman spectra of the natural uranyl selenite derriksite, complemented by its infrared spectra. The paper is a part of systematic vibrational spectroscopic research of secondary minerals formed in the oxidation zone, inclusive uranyl minerals originating during hydration–oxidation weathering of primary uranium minerals, such as uraninite. Raman spectroscopy was proven most useful for the characterization of secondary uranyl containing minerals. In order to identify and characterize the Raman and infrared spectra of derriksite, this research reports the Raman and infrared spectrum of derriksite and relates the spectra of derriksite to the structure of the mineral.

Experimental

Mineral

For the development of this work, one single crystal of derriksite was chosen for our investigation. Sample was obtained from the collection of the Geology Department of the Federal University of Ouro Preto, Minas Gerais with sample code SAB-098. The crystal is deep green and transparent, with up to 2.0 mm in length and occurs in association with malachite. The studied sample is from Musonoi Mine, Katanga, Democratic Republic of Congo and can be considered a type material.

The chemical analyses of the mineral have been made. These are included in Supplementary information.

Raman microprobe spectroscopy

Crystals of derriksite were placed on a polished metal surface on the stage of an Olympus BHSM microscope, which is equipped with 10×, 20×, and 50× objectives. The microscope is part of a Renishaw 1000 Raman microscope system, which also includes a monochromator, a filter system and a CCD detector (1024 pixels). The Raman spectra were excited by a Spectra-Physics model 127 He–Ne laser producing highly polarized light at 633 nm and collected at a nominal resolution of 2 cm^{-1} and a precision of ±1 cm^{-1} in the range between 200 and 4000 cm^{-1}. Repeated acquisitions on the crystals using the highest magnification (50×) were accumulated to improve the signal to noise ratio of the spectra. Raman Spectra were calibrated using the 520.5 cm^{-1} line of a silicon wafer. The Raman spectrum of at least 10 crystals was collected to ensure the consistency of the spectra.

Infrared spectroscopy

Infrared spectra were obtained using a Nicolet Nexus 870 FTIR spectrometer with a smart endurance single bounce diamond ATR cell. Spectra over the 4000–525 cm^{-1} range were obtained by the co-addition of 128 scans with a resolution of 4 cm^{-1} and a mirror velocity of 0.6329 cm/s. Spectra were co-added to improve the signal to noise ratio. The infrared spectra are given in the supplementary information.

Spectral manipulation such as baseline correction/adjustment and smoothing were performed using the Spectracalc software package GRAMS (Galactic Industries Corporation, NH, USA). Band component analysis was undertaken using the Jandel 'Peakfit' software package that enabled the type of fitting function to be selected and allows specific parameters to be fixed or varied accordingly. Band fitting was done using a Lorentzian–Gaussian cross-product function with the minimum number of component bands used for the fitting process. The Gaussian–Lorentzian ratio was maintained at values greater than 0.7 and fitting was undertaken until reproducible results were obtained with squared correlations of r^2 greater than 0.995.

Results and discussion

The Raman spectrum of derriksite over the full wavenumber range is illustrated in Fig. 1a. This figure displays the position and relative intensities of the Raman bands of derriksite. It may be observed that there are large parts of the spectrum where no intensity is found; therefore the spectrum is subdivided into sections based upon the type of vibration being studied. The infrared spectrum of derriksite over the full wavenumber range is illustrated in Fig. 1b. This spectrum shows the position and relative intensities of the infrared bands of derriksite. The Raman spectrum of derriksite over the 700 to 1400 cm^{-1} spectral range is reported in Fig. 2a. The infrared spectrum of derriksite over the 600 to 1400 cm^{-1} spectral range is reported in Fig. 2b. The Raman spectra of derriksite over the 300 to 700 cm^{-1} and 100 to 300 cm^{-1} spectral ranges are reported in Fig. 3. The Raman and infrared spectra of the OH stretching region (2600–4000 cm^{-1}) are shown in Fig. 4. The Raman and infrared spectra in the water bending region (1300–1800 cm^{-1}) are given in Fig. 5.

The free linear uranyl group $(UO_2)^{2+}$, symmetry $D_{\infty h}$, has four normal vibrations, but only three fundamentals: the ν_1 symmetric stretching vibration, Raman active (approximately 900–700 cm^{-1}), the ν_2 (δ) doubly degenerate bending vibration, infrared active (approximately 300–200 cm^{-1}), and the ν_3 antisymmetric stretching vibration, infrared active (approximately 1000–850 cm^{-1}). Distortion of the uranyl group or change in the local symmetry can result in the removal of the degeneracy and therefore Raman activation of the ν_2 mode and infrared activation of the ν_1 mode [24].

The chemistry of the selenite ion and selenite containing compounds resembles the chemistry of the sulphite ion and its compounds. The polyhedron of the selenite ions is similar to that of sulphite ions, which is trigonal pyramid with one vacant orbital
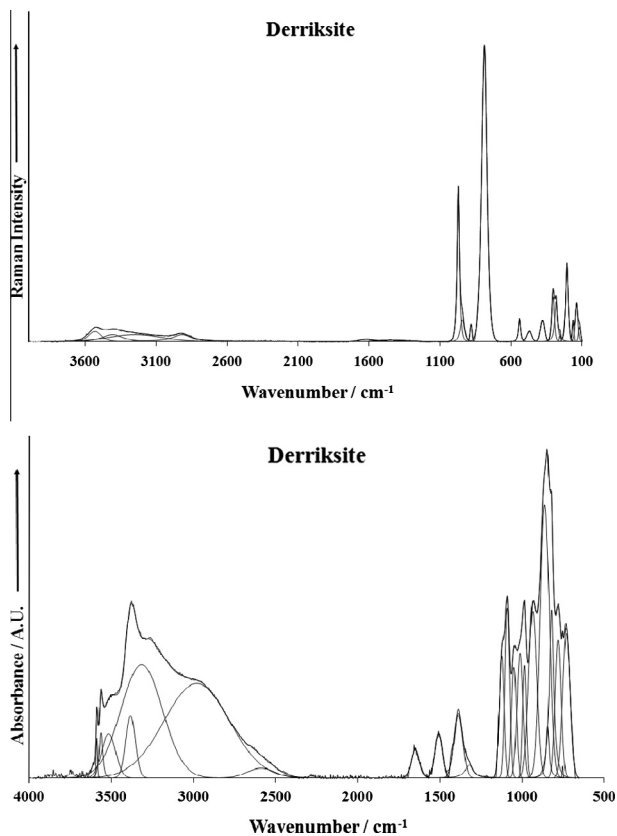
Fig. 1. (a) Raman spectrum of derriksite over the 100 to 4000 cm^{-1} spectral range. (b) Infrared spectrum of derriksite over the 500 to 4000 cm^{-1} spectral range.
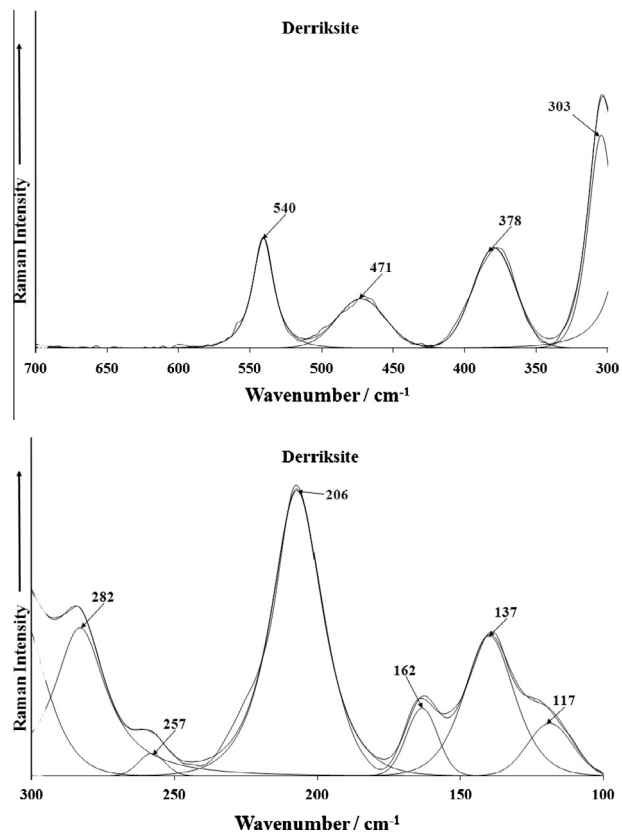

Fig. 3. (a) Raman spectrum of derriksite over the 300 to 800 cm^{-1} spectral range. (b) Raman spectrum of derriksite over the 100 to 300 cm^{-1} spectral range.
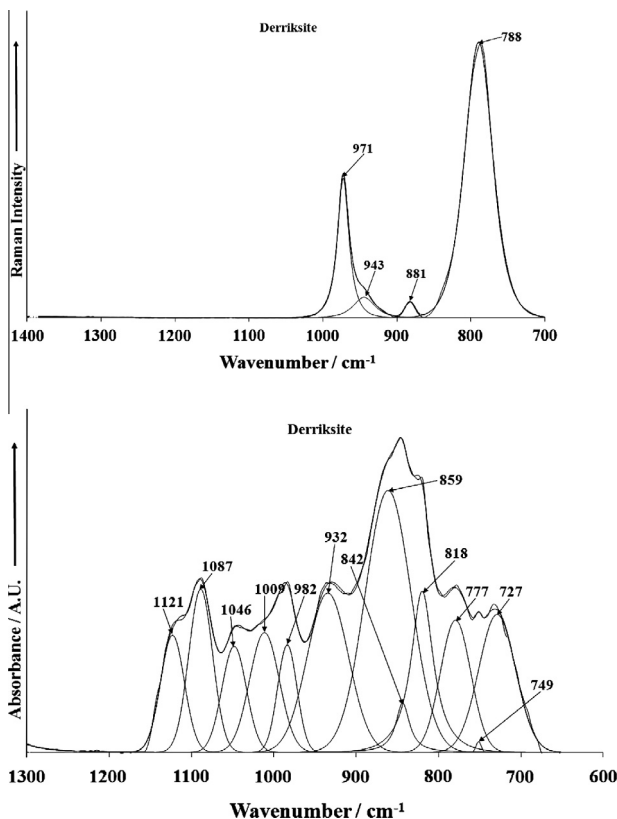

Fig. 2. (a) Raman spectrum of derriksite over the 800 to 1400 cm^{-1} spectral range. (b) Infrared spectrum of derriksite over the 500 to 1300 cm^{-1} spectral range.
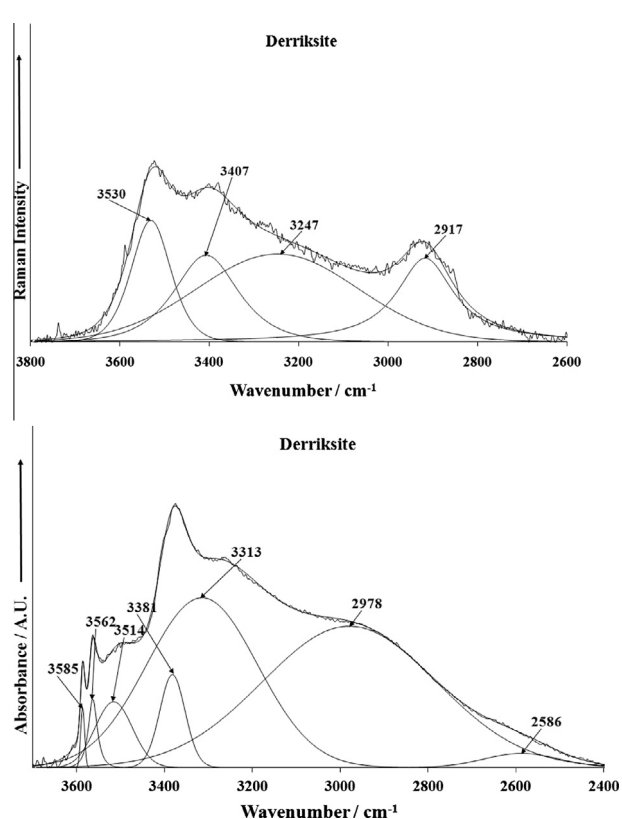

Fig. 4. (a) Raman spectrum of derriksite over the 2600 to 4000 cm^{-1} spectral range. (b) Infrared spectrum of derriksite over the 2600 to 4000 cm^{-1} spectral range.
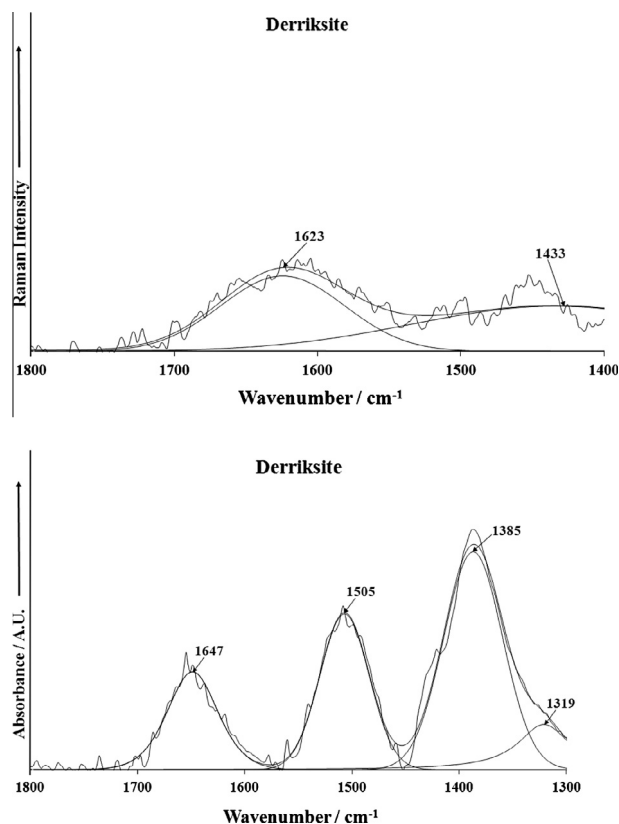
Fig. 5. (a) Raman spectrum of derriksite over the 1300 to 1800 cm^{-1} spectral range. (b) Infrared spectrum of derriksite over the 1300 to 1800 cm^{-1} spectral range.

thus making C_{3v} symmetry [25]. The selenite ion (SeO$_3$)$^{2-}$ has four fundamentals: the v_1 symmetric stretching vibrations (approximately 790–806 or 760–855 cm^{-1}, the v_2 symmetric bending vibration (approximately 430–461 cm^{-1}), the v_3 doubly degenerate antisymmetric stretching vibration (714–769 or 680–775 cm^{-1}), and the v_4 doubly degenerate antisymmetric bending vibration (approximately 387–418 cm^{-1}). All vibrations are Raman and infrared active [26–29]. The degeneracy of the antisymmetric v_3 and v_4 modes of the (SeO$_3$)$^{2-}$ may be removed due to the lowering of its site symmetry in the unit cell.

In the crystal structure of orthorhombic derriksite (S.G. $Pn2_1m = C_{2v}^7$, a 5.570(2), b 19.088(8), c 5.965 Å), there are one symmetrically distinct U^{6+}, two symmetrically distinct Se^{4+}, three symmetrically distinct Cu^{2+}, six symmetrically distinct O^{2-} and four symmetrically distinct OH$^-$, $Z = 2$ [11].

Raman band at 788 cm^{-1} and an infrared band at 818 cm^{-1} are assigned to the v_1 (UO$_2$)$^{2+}$ symmetric stretching vibrations, however, both bands coincide with the v_1 (SeO$_3$)$^{2-}$ symmetric stretching mode. No Raman band was attributed to the v_3(UO$_2$)$^{2+}$ antisymmetric stretching vibration. An infrared band at 859 cm^{-1} is assigned to the v_3(UO$_2$)$^{2+}$ antisymmetric stretching vibration. Approximate U–O bond lengths in uranyl were calculated with two empirical relations using wavenumbers of the stretching uranyl vibrations, i.e. R$_{U-O}$ = 0.575 + 106.5$v_1^{-2/3}$Å, and R$_{U-O}$ = 0.804 + 91.41$v_3^{-2/3}$Å, published by Bartlett and Cooney [30]. Obtained calculated U–O bond lengths (Å/cm^{-1}) 1.823/788, 1.793/818 and 1.816/859 are close to the average U–O bond length 1.795 Å, inferred from the X-ray single crystal structure of derriksite [10,11]. Raman band at 812 cm^{-1} was assigned to the v_1 (UO$_2$)$^{2-}$ in marthozite [29] and haynesite [17]. In demesmaekerite, Raman band at 822 cm^{-1} and an infrared band at 819 cm^{-1} were attributed to the v_1 (UO$_2$)$^{2+}$ symmetric stretching vibration and an infrared band at 878 cm^{-1} to the (UO$_2$)$^{2+}$ antisymmetric

stretching vibration. Infrared bands at 879 and 820 cm^{-1} in the spectrum of marthozite [29] and at 898 and 815 cm^{-1} in the spectrum of piretite were attributed to the v_3 (UO$_2$)$^{2+}$ and v_1 (UO$_2$)$^{2+}$, respectively. Chukanov et al. [9] assigned the infrared band at 901 cm^{-1} in the spectrum of larisaite to the uranyl stretching vibration.

Raman band at 788 and infrared bands at 777 and 818 cm^{-1} may be attributed to the v_1 (SeO$_3$)$^{2-}$ symmetric stretching vibrations coinciding with the v_1 (UO$_2$)$^{2-}$ symmetric stretching vibrations, and infrared bands at 727 and 749 to the doubly degenerate v_3 (SeO$_3$)$^{2-}$ antisymmetric stretching vibrations. Raman band at 540 cm^{-1} is probably connected with the libration modes of water molecules or hydroxyl ions and/or to the v (U–O$_{ligand}$) vibrations. Raman bands at 303 cm^{-1} and 378 and 471 cm^{-1} are attributed to the v_2 and v_4 (SeO$_3$)$^{2-}$ vibrations, respectively. The v_2 (δ) (UO$_2$)$^{2+}$ bending vibrations were observed in the Raman spectrum at 282 and 257 cm^{-1}, while the bands at 206, 162, 135 and 117 cm^{-1} may be assigned to the lattice vibrations. Infrared spectrum of Sr[(UO$_2$)$_3$O$_2$(SeO$_3$)$_2$](H$_2$O)$_4$, observed in this region is as follows: 909 cm^{-1} (v_3 (UO$_2$)$^{2+}$), 865 cm^{-1} (v_1 (UO$_2$)$^{2+}$, 839, 814, 725 and 615 cm^{-1} [31]. The structure of this synthetic compound, however, contains two-dimensional [(UO$_2$)$_3$(O$_2$)(SeO$_3$)$_2$]$^{2-}$ sheets with the same phosphuranylite anion sheet topology as found in the structures of guilleminite, marthozite and larisaite, and expected also in piretire and haynesite. This topology differs from that of derriksite and also demesmaekerite.

Infrared bands in the 982 to 1121 cm^{-1} and Raman band at 971 cm^{-1} are assigned to the δ Cu–OH bending vibrations. In this region, infrared bands were observed in demesmaekerite (infrared 1033, 1049, 1090, 1122, 1167 and 1194 cm^{-1}), marthozite (1120, 1096, 1049 and 1027 cm^{-1}) [29], larisaite (1044 and 1095 cm^{-1}) [9] and haynesite (1168, 1116, 1081 and 1036) [17,27,32], which may be also attributed to the δ M–OH bending vibrations and/or combination bands. Chukanov et al. [9] assume that some of these bands together with some other at different wavenumbers may be connected with the (H$_3$O)$^+$ bending vibrations and that especially haynesite contains hydroxonium cations and may be formulated as (H$_3$O)$_2$[(UO$_2$)$_3$(OH)$_4$(SeO$_3$)$_2$]·H$_2$O. However, marthozite does not contain any hydroxonium ions and some bands in the mentioned region may be also observed. Chukanov et al. [9] assigned a band at 1732 cm^{-1} in the infrared spectrum of haynesite to the doubly degenerate bending vibration of hydroxonium ions. It is more probable that this infrared band may be attributed to the combination ($v_1 + v_3$ (UO$_2$)$^{2+}$) band, and some bands in the region 1000–1200 cm^{-1} may be connected with the combination ($v_1 + v_2$ (UO$_2$)$^{2+}$ and/or ($v_3 + v_2$ (UO$_2$)$^{2+}$) bands. Frost et al. did not infer the presence of hydroxonium ions in the structure of haynesite in their Raman spectroscopic study of the uranyl selenite mineral haynesite [17]. In the case of derriksite, Raman bands at 881 and 943 cm^{-1} and infrared bands at 842 and 932 cm^{-1} may be related to the libration modes of water molecules and/or to the δ Cu–OH bending vibrations.

Infrared bands observed at 1319, 1385, 1505 cm^{-1} and Raman band at 1433 cm^{-1} may be connected with overtones and/or combination bands. Raman band at 1623 cm^{-1} and the infrared band at 1647 cm^{-1} are assigned to the δ bending vibration of hydrogen bonded water molecules.

Raman bands at 3530 and 3407 cm^{-1} and infrared bands at 3585, 3562, 3514 and 3381 cm^{-1} are attributed to the v OH stretching vibrations of only weakly hydrogen bonded hydroxyls and those at 3247 and 2917 cm^{-1} and 3313 and 2978 cm^{-1}, respectively, to the v OH stretching vibrations of hydrogen bonded water molecules. An infrared band at 2586 cm^{-1} may be connected with a combination band or an overtone. Approximate O–H···O hydrogen bond lengths inferred from observed wavenumbers vary in the range 3.2–2.64 Å [33]. These values are close those inferred

from the X-ray single crystal structure analysis of derriksite [10,30]. Observed number of the infrared bands in the region of v OH stretching vibrations proves the presence of structurally non-equivalent hydroxyls and structurally nonequivalent water molecules (water of crystallization) in the derriksite unit cell ($Z = 2$).

Conclusions

(1) Raman and infrared spectra of uranyl selenite mineral derriksite were measured, tentatively interpreted and partly compared with the spectra of demesmaekerite, marthozite, larisaite, haynesite, piretite and synthetic $Sr[(UO_2)_3O_2(SeO_3)_2]\cdot(H_2O)_4$.

(2) The presence of symmetrically distinct hydrogen bonded molecule of water of crystallization and hydrogen bonded hydroxyls was inferred from the spectra.

(3) Approximate U–O bond lengths in uranyls and O–H⋯O hydrogen bond lengths were inferred from the Raman and infrared spectra with empirical relations by Bartlett and Cooney [30] and Libowitzky [33], respectively [34–36]. They are close to the U–O and O–H⋯O lengthes calculated on the basis of X-ray single crystal structure of derriksite [11].

Acknowledgements

Appendix A. Supplementary material

Supplementary data associated with this article can be found, in the online version, at http://dx.doi.org/10.1016/j.saa.2013.08.026.

References

[1] M. Koskenlinna, Structural Features of Selenium(IV) Oxoanion Compounds, Thesis, Helsinky University of Technology, Espoo, 1996.
[2] L.B. Serezhkina, R.K. Rastsvetaeva, V.N. Serezhkin, Koord. Khim. 16 (1990) 1327–1339 (in Russian).
[3] P.C. Burns, Am. Mineral. 82 (1997) 1176–1186.
[4] P.C. Burns, Can. Mineral. 43 (2005) 1839–1894.
[5] P.C. Burns, Mater. Res. Soc. Symp. Proc. 802 (2004) 89–100.
[6] P.C. Burns, Rev. Mineral. 38 (1999) 23–90.
[7] R. Finch, T. Murakami, Rev. Mineral. 38 (1999) 91–179.
[8] J.F.W. Bowles, Handbook of mineralogy, in: J.W. Anthony, R.A. Bideaux, K.W. Bladh, M.C. Nichols (Eds.), Borates, Carbonates, Sulfates, vol. 5, Mineral Data Publishing, Tuscon, Arizona, USA, 2003.
[9] N.V. Chukanov, D.Y. Pushcharovsky, M. Pasero, S. Merlino, A.V. Barinova, S. Moeckel, I.V. Pekov, A.E. Zadov, V.T. Dubinchuk, Eur. J. Mineral. 16 (2004) 367–374.
[10] R.P.F. Cesbron, T. Verbeek, Bull. Soc. Fr. 94 (1972) 534–537.
[11] D. Ginderow, F. Cesbron, Cryst. Struc. Commun. C39 (1983) 1605–1607.
[12] D. Ginderow, F. Cesbron, Cryst. Struc. Commun. C39 (1983) 824–827.
[13] M.A. Cooper, F.C. Hawthorne, Can. Mineral. 33 (1995) 1103–1109.
[14] M.A. Cooper, F.C. Hawthorne, Can. Mineral. 39 (2001) 797–807.
[15] M. Deliens, P. Piret, Haynesite, Can. Mineral. 29 (1991) 561–564.
[16] R. Vochten, N. Blaton, O. Peeters, M. Deliens, Can. Mineral. 34 (1996) 1317–1322.
[17] R.L. Frost, M.L. Weier, B.J. Reddy, J. Čejka, J. Raman Spectrosc. 37 (2006) 816–821.
[18] R.L. Frost, K.L. Erickson, M.L. Weier, O. Carmody, J. Čejka, J. Mol. Struc. 737 (2005) 173–181.
[19] R.L. Frost, M.L. Weier, T. Bostrom, J. Čejka, W. Martens, Neues Jahrb. Mineral. 181 (2005) 271–279.
[20] R.L. Frost, O. Carmody, K.L. Erickson, M.L. Weier, J. Čejka, J. Mol. Struc. 703 (2004) 47–54.
[21] R.L. Frost, D.A. Henry, K. Erickson, J. Raman Spectrosc. 35 (2004) 255–260.
[22] R.L. Frost, M.L. Weier, M.O. Adebajo, Thermochim. Acta 419 (2004) 119–129.
[23] R.L. Frost, K.L. Erickson, J. Čejka, B.J. Reddy, Spectrochim. Acta A61 (2005) 2702–2707.
[24] J. Čejka, Rev. Mineral. 38 (1999) 521–622.
[25] N.N. Greenwood, A. Earnshaw, Chemistry of Elements, Pergamon Press, Oxford, 1984.
[26] J. Čejka, J. Sejkora, R.L. Frost, E.C. Keeffe, J. Raman Spectrosc. 40 (2009) 1521–1526.
[27] R.L. Frost, J. Čejka, Spectrochim. Acta A71 (2009) 1959–1963.
[28] R.L. Frost, J. Čejka, M.J. Dickfos, J. Raman Spectrosc. 40 (2009) 476–480.
[29] R.L. Frost, J. Čejka, E.C. Keeffe, M.J. Dickfos, J. Raman Spectrosc. 39 (2008) 1413–1418.
[30] J.R. Bartlett, R.P. Cooney, J. Mol. Struc. 193 (1989) 295–300.
[31] P.M. Almond, T.E. Albrecht-Schmitt, Am. Mineral. 89 (2004) 976–980.
[32] R. Frost, B. Jagannadha Reddy, M. Dickfos, J. Near Infrared Spectrosc. 16 (2008) 455–469.
[33] E. Libowitzky, Monatshefte für Chem. 130 (1999) 1047–1059.
[34] R. Tali, V.V. Tabachenko, L.M. Kovba, Zh. Neorg. Khim. 38 (1993) 1450–1452 (in Russian).
[35] D.Y. Pushcharovsky, R.K. Rastsvetaeva, H. Sarp, J. Alloys Compd. 239 (1996) 23–26.
[36] H. Yang, R.A. Jenkins, R.M. Thompson, R.T. Downs, S.H. Evans, E.M. Bloch, Am. Mineral. 97 (2012) 197–202.